

LIGO SURF Final Report: Developing a Coherent Search Algorithm to Identify Continuous Phase Modulated Gravitational Wave Sources

Camilla Compton 23rd September 2016

Mentors Dick Gustafson and Keita Kawabe

A coherent sideband search algorithm for identifying continuous, phase modulated gravitational waves from LIGO data has been further developed. Phase modulation occurs due to a Doppler shift of the gravitational wave frequencies, which are produced by rotationally asymmetric neutron stars, when the stars are moving in binary systems. The studied algorithm searches over the frequency of the star's rotation, the period about it's binary companion, the phase between these, and the phase modulation index, which is dependent on the star's period and the separation between it and it's companion. The method is successful in identifying correct input parameters from simulated data; there are some limitations in finding modulation frequency, due to characteristics of the discrete Fourier transform, which are yet to be solved.

Contents

1	Introduction	1
1.1	Neutron Stars	1
2	The Search Algorithm	1
2.1	Expected Values of Search Parameters	2
3	Results	2
3.1	Testing across Input Parameters	3
3.2	The Effects of the Discrete Fourier Transform	6
4	Conclusion	7
A	Derivation of Search Algorithm	8
B	The Discrete Fourier Transform	9

1 Introduction

A search algorithm for continuous gravitational waves (CW), particularly those produced by binary neutron star systems, has been further developed from Deanna Emery's work in 2015 and tested [1]. The signal this search aims to find is phase modulated by a Doppler shift due to the orbit of the binary system while the it is steadily rotating.

Although there are already many methods which have been designed to identify continuous gravitational waves, they are still under development and, somewhat surprisingly, no continuous wave (CW) signals have yet been found. The method behind the search algorithm described is a coherent search over the frequency sidebands in a phase modulated wave. The aim of this paper is to describe the theory behind this search. The algorithm is coherent, meaning it should be more robust against noise than other CW methods which use magnitude of frequency information. This is an important factor that must be considered, along with search accuracy, and computation time needed, when evaluating the success of the search.

The described search offers a new method of CW gravitational wave detection which would increase the chance of binary neutron star identification if the method could be proved successful.

1.1 Neutron Stars

Neutron stars (NS) are the mass of 1.3 to 2.5 solar masses but are only a city-sized sphere of around 20 kilometres across [6]. This incredibly high density means that NS have very large amounts of gravity associated with them. Generally, NS are spinning, due to their formation and how they exist, therefore if they are spherically asymmetric gravitational waves will be given of as they rotate. This is due to the quadrupole moment of mass distribution changing. It is expected that NS will be asymmetric enough that LIGO will be able to observe them.

Astronomers have found fewer than 2,000 pulsars, but near a billion NS are expected to exist in our Milky Way Galaxy [6]. Further, over 50% of stars are confirmed to be in binary or higher relationships, with the expected number to be nearer 80% [7]. Therefore, if NS do emit gravitational waves at the expected amplitudes LIGO should be able to detect them, and a lot of them.

2 The Search Algorithm

The phase modulation of the expected signal causes sidebands in frequency space. this is due to the frequency drifting from the central frequency when it is Doppler shifted different amounts from the stars circular orbit. For example, if the orbit was in the plane of the earth, the frequency measured by the earth would be only the same as the emitted frequency when the star is travelling exactly perpendicular to the earth, when it is moving towards or away from the earth it would be measured as a larger or smaller frequency. Mathematically, this gives discrete sidebands at values separated by the modulation frequency about the central carrier frequency . These sidebands and their phase are utilised in the coherent search technique which has been developed.

The expected phase modulated gravitational wave is of the form

$$d(t) = e^{i(\omega_0 t + \Gamma \cos(\Omega t))}. \quad (1)$$

It is dependant on carrier frequency, ω , modulation frequency, Ω , and modulation index, Γ . Additionally, there are phase factors between ω and Ω which have not been included here. This is a standard phase modulated wave form which is physically equivalent to frequency modulation, however, the Γ factor should not be confused with the modulation index for frequency modulation.

By rearrangement, using the Jacobi-Anger expansion and taking the Fourier transform of both sides of the equation, the search algorithm's key equation,

$$\delta(\omega - \omega_0) = J_0(\Gamma)D(\omega) + \sum_{n=1}^{\infty} e^{-in\frac{\pi}{2}} J_n(\Gamma)(D(\omega - n\Omega) + D(\omega + n\Omega)) \quad (2)$$

can be obtained [1]. $J_n(\Gamma)$ is the value of the n th Bessel function at Γ and $D(\omega)$ is the Fourier transform of the data, $d(t)$, at ω . A full explanation of this derivation can be seen in Appendix A.

The search implemented calculates the right side of equation 2 by using MATLAB's built in FFT function to find $D(\omega)$ and the built in Bessel terms function in MATLAB to find the J_n terms. It is expected that in

the future J_n terms can be calculated once and stored to save computation time. The calculation is repeated over varying values of ω , Ω , and Γ in a specified range. How fine the search steps over the specified range of the search parameter is dependant on the parameter and discussed in Section 3.1.

Theoretically, once Equation 2 is completed for all values in the search, a non-zero value should be only be observed at $\omega = \omega_0$. This is represented graphically as a delta function when the magnitude of the calculated summation is plotted as a surface for each search value of ω and Ω . This is generally observed, as displayed by the peak in figure 1. These plots would be recreated for each value of Γ and the largest magnitude point taken to be correct. Figure 1 additionally shows undesirable features which are the artefacts discussed in section 3.

Noise is neglected here but it's addition has minimal impact to the theory behind the algorithm.

2.1 Expected Values of Search Parameters

The expected values of the search parameters were found by reviewing known neutron stars (NS) in binary systems, NS-NS pairs were mainly studied [2] [3].

The carrier frequency of the gravitational waves (twice the frequency that the NS spins), ω , are expected to be in the range 0.72 to 500Hz with an estimated average of 70Hz. The LIGO detector only has it's best sensitivity in the range 50 to 1500Hz, therefore NS's emitting gravitational waves with frequencies below 50Hz will not be detected.

The range of modulation frequency, Ω , is 10^{-7} to 10^{-4} Hz with an estimated average of 2.5×10^{-5} Hz. This equates to an orbit time of around 11 hours.

The modulation index, Γ , can be derived by considering how the Doppler shift of the star changes during it's orbit with the companion to be

$$\Gamma = \frac{\omega R}{c}. \quad (3)$$

R is the distance to the NS to the pair's centre of mass and c is the speed of light. The range of Γ has been found to be from 100 to the maximum value of 100,000: however the average was estimated to be round 1000.

3 Results

In 2015 Deanna Emery created the basic search that returned the 'perfect' delta function-like peak that was expected theoretically. This can be seen in Figure 1, however the search additionally returned unwanted peaks that were thought to be due to the discrete nature of the search [1]. These signals have since been found to be directly due to the summation method of the search: if an FFT bin which is expected to include a signal is empty, the overall result is non-zero if there are any signals in other bins where the FFT sidebands are expected. This effect should be greatly reduced in comparison to other non-coherent methods, however a direct comparison has not yet been made. In certain cases, discussed below, this is non-negligible.

Unwanted lines of around 10-20% of the peak magnitude can be seen at constant values of ω_0 and the nearby sidebands: $\omega = \omega_0 \pm n\Omega$ for small n , as displayed in figure 1. This is because if the search takes ω to be one of these values there will always have some power in the summation from the $D(\omega)$ term lying on a peak.

There is additionally signals measured at constant gradients

$$\frac{d\omega}{d\Omega} = \frac{1}{m}$$

where m is an integer. These eventually form crosses [4]. This is due to the $\delta(\omega - \omega_0 - n\Omega - m\Omega')$ factor in the Fourier transformed signal leading to some power being steadily counted in the summation [5]. More practically, this can be thought of as a shift down in Ω , decreasing the spacing between the template of the bins we sum over, while an equal shift up in ω , which shifts the entire coherent template higher. Overall, when this is repeated, one sideband is always included in the sum and thus a linear undesired signal is seen which appears with a constant gradient in $\frac{\omega}{\Omega}$.

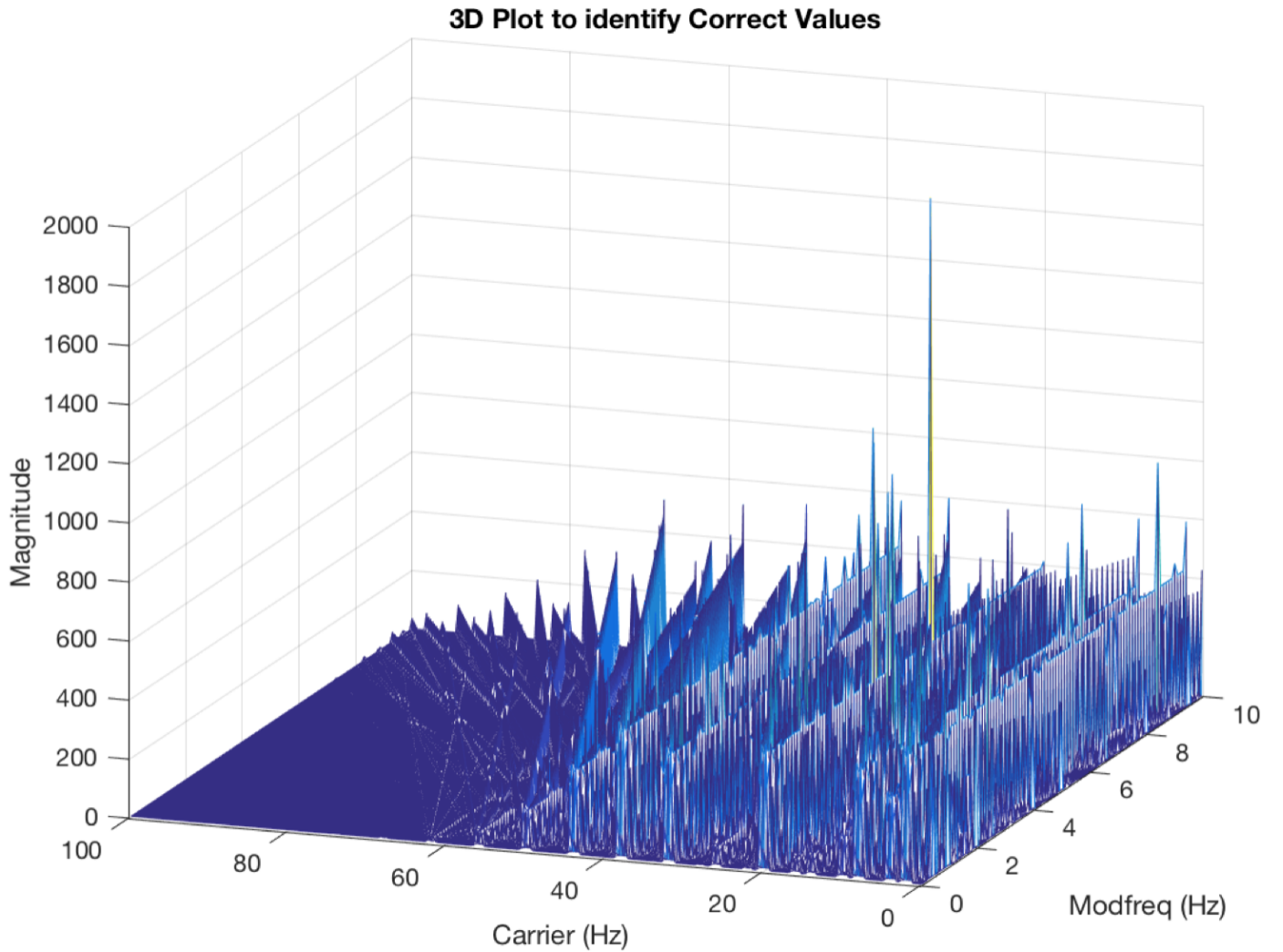


Figure 1: The search of a phase modulated signal with $\omega = 20\text{Hz}$, $\Omega = 6\text{Hz}$, $\Gamma = 4$, sample time = 10s and sample frequency = 500Hz. Extra undesired signals can be seen as stripes at values of constant ω and at constant $\frac{\omega}{\Omega}$ integer gradients due to the method of power summation used.

The ‘perfect’ peak was surprisingly found to completely disappear when input parameters which were irrational numbers were used. In fact, this occurred whenever the Ω input was not centred on a bin: the precise data points in the FFT frequency space which are spaced by $\frac{1}{T}\text{Hz}$. This was not noticed previously as the algorithm was only tested with rounded values of input parameters. This significantly slowed down progress as it became apparent the algorithm was not yet ready to be tested along side other CW algorithms or with more realistic data.

3.1 Testing across Input Parameters

It is important to understand how well the search works with realistic input parameters especially as it has been identified that non bin-centred parameters cause problems. To investigate this, the search was repeated while stepping through 10,000 different input parameters over the width of one bin. The magnitude of the result of the summation (equation 2), returned as a peak at the known parameter location, gives a measure of the success of the search: the larger the peak the more it will contrast to any noise and artefacts.

A smooth decrease in the magnitude of the summation (the peak) is seen when the carrier frequency’s value is moved away from the centre of a FFT frequency space bin. The search is being done at multiples in ω of $\frac{1}{T}$ only. This is displayed in Figure 2, where the maximum (normalised) peak value decreases from 1, when ω is at a multiple of 0.01Hz which is the centre of a FFT frequency bin, to a minimum of 0.63 when ω is exactly between bins. This is a reasonable decrease as gives an average magnitude of the calculated summation of over

0.8. Further, It is thought that the amount the magnitude decreases by can be reduced if interpolation or if a finer search over ω is used in the future.

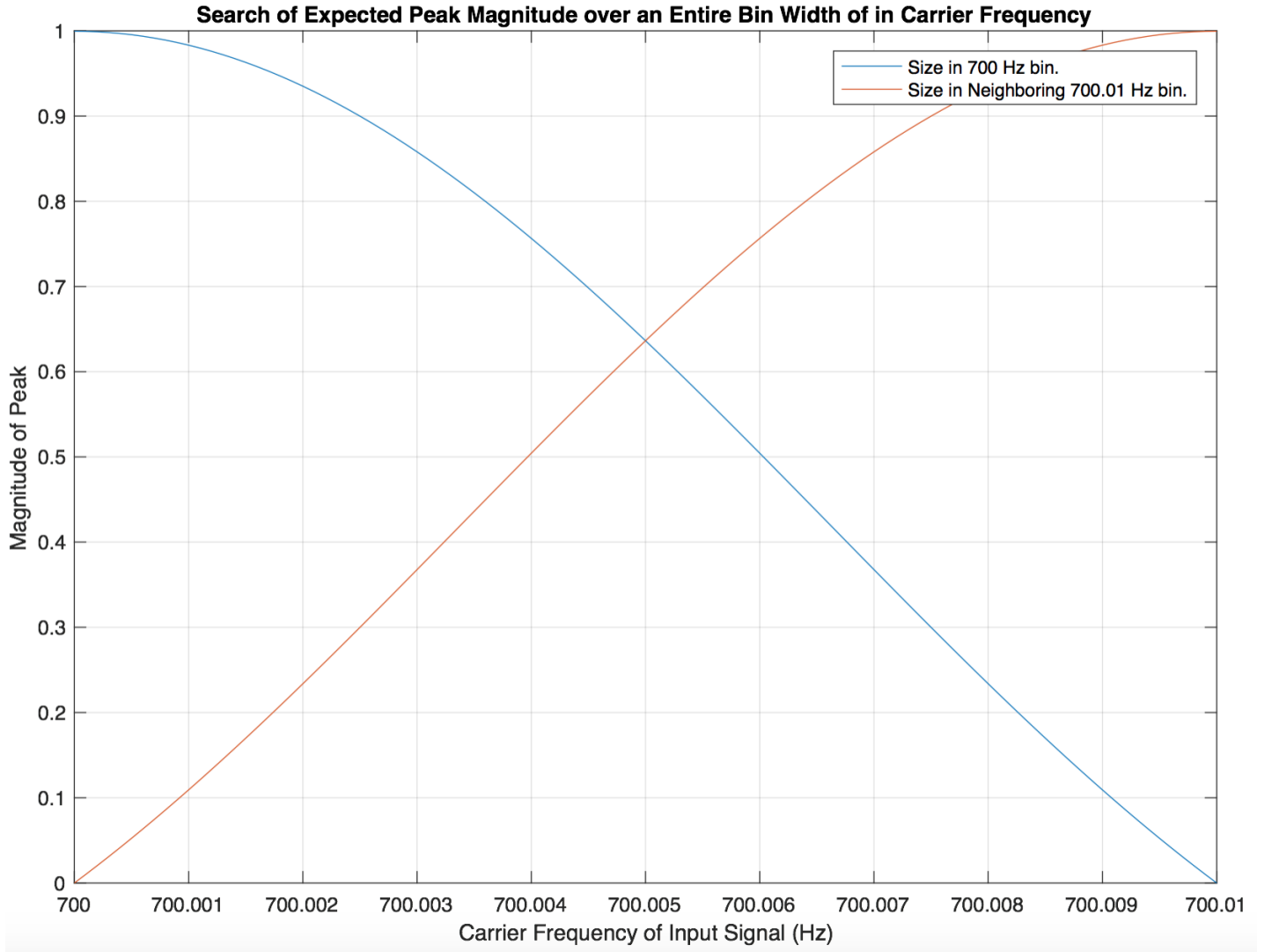


Figure 2: The magnitude of the peak returned by the search for fixed values of $\Omega = 0.3\text{Hz}$ and $\omega = 700$ (blue) and 700.01Hz (red), normalised to one, for 10,000 different non bin-centred input values of ω between 700 and 700.01Hz when $\Omega = 0.3\text{Hz}$. It can be seen that when the input ω is equal to the search value, thus bin-centred, 100% of the signal is extracted: at 700 and 700.01Hz . Otherwise some signal is lost and a non-zero value is counted by the neighbouring bin.

When the same search is completed by stepping over Ω , the result is drastically different as seen in Figure 3. The search is being done at Ω multiples of $\frac{1}{T}$ only. Here, the search only returns the expected normalised peak very close to the bin-centred value. The result of the search (magnitude of peak) is over 0.5 only 1% of the time and it can be seen to average below 0.05. This is not viable for a search as so much of the power is generally lost, only 1% of events would be seen.

Small peaks which can be seen in Figure 3 around 0.33Hz are related to harmonics of the search values, meaning higher proportions of power is found in the FFT bins at the values of the search and thus the summation magnitude is larger.

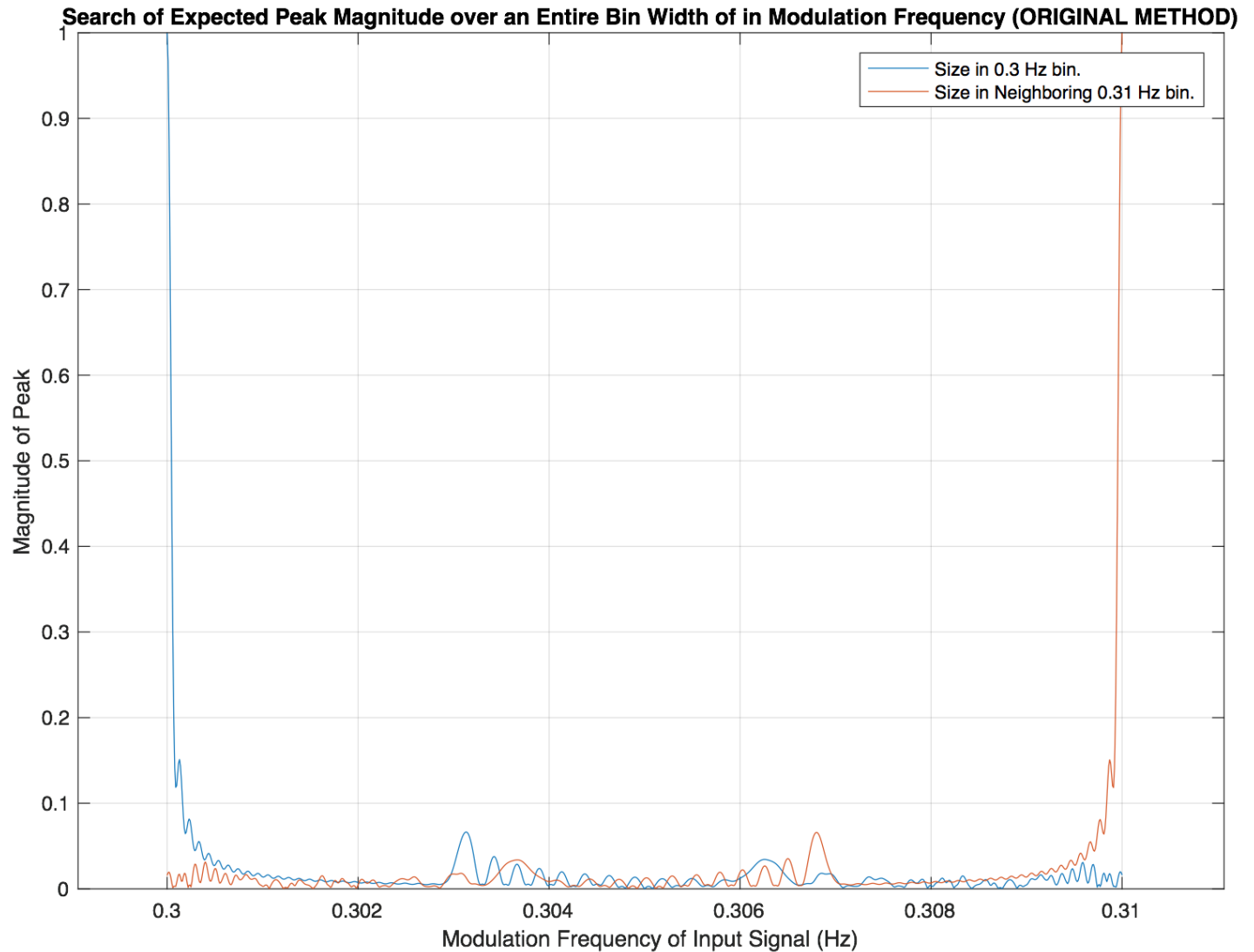


Figure 3: The magnitude of the peak returned by the search for fixed values of $\omega = 700\text{Hz}$ and $\Omega = 0.3$ (blue) and 0.31Hz (red), normalised to one, for 10,000 different non bin-centred input values of Ω between 0.3 and 0.31Hz when $\omega = 700\text{Hz}$. It can be seen that when Ω of the input signal is equal to the search value, thus bin-centred, 100% of the signal is extracted: at 0.3 and 0.31Hz . Otherwise the majority of the signal is lost.

The search stepping over the Ω input was then repeated by searching for values of Ω with a density increased by a factor of 1000. Computationally, the FFT frequency bins chosen to be in the summation were then not exact, be found by rounding multiples of the, now more exact, Ω search values. The magnitude of the largest peak in a small sample of ω and Ω searches around the correct parameters was then plotted in Figure 4. This shows a large improvement to Figure 3, with an average magnitude of 0.5, however a 1000 fold increase in computational time required to compute the search. Further investigations should be undertaken to find the optimum spacing.

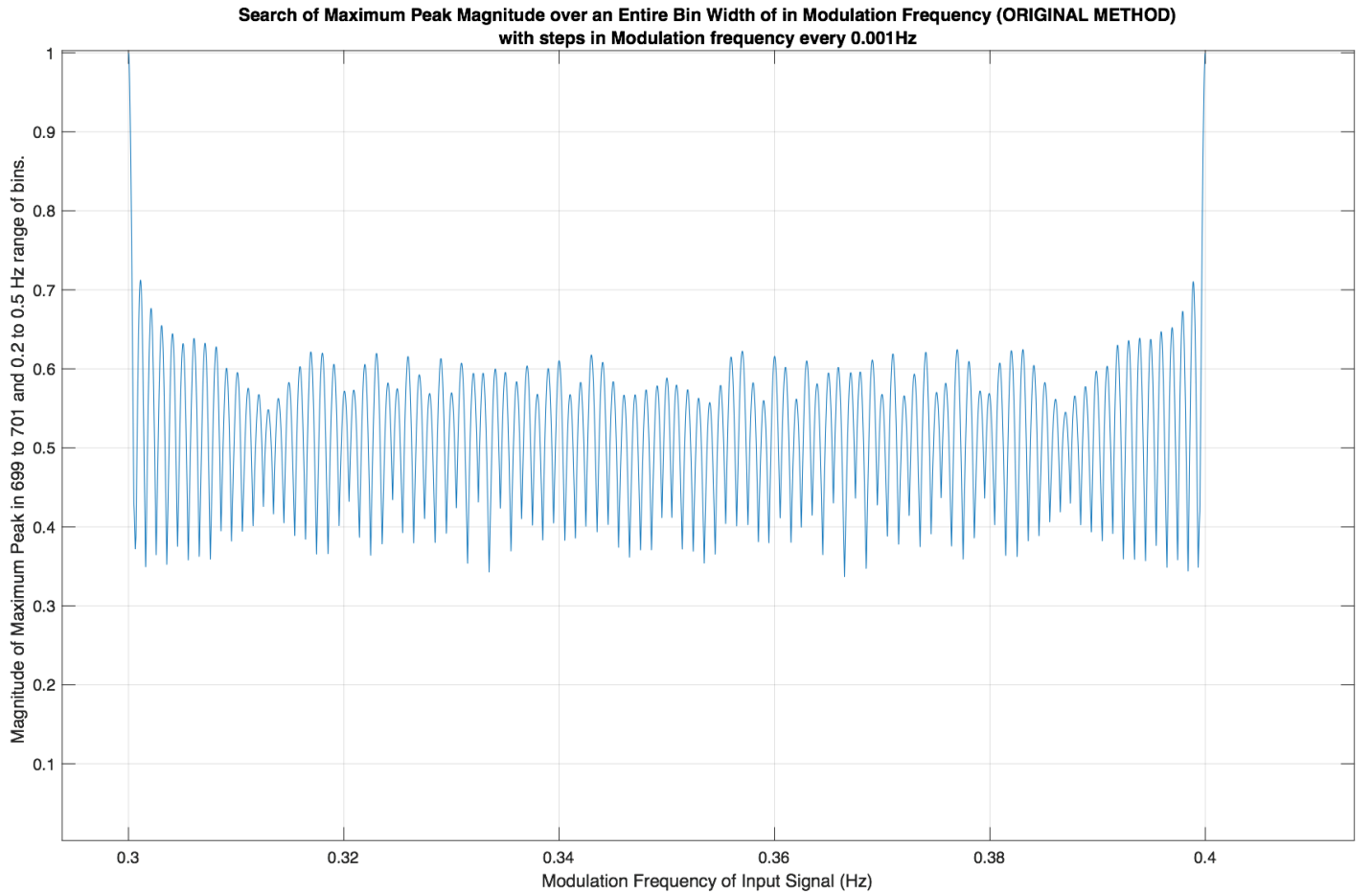


Figure 4: The magnitude of the highest peak returned by the search for fixed values of ω and Ω , normalised to one, for 10,000 different non bin-centred input values of Ω between 0.3 and 0.31Hz when $\omega = 700\text{Hz}$. The difference between this graph and that in figure 3 is that the search is now done over a factor of 1000 more values of Ω , therefore the average magnitude of the signal is 0.5: half the power on average is lost. Note that the scale is larger than in figure 3 due to a smaller T being used to reduce computational time, thus each FFT bin is a factor of 10 wider.

3.2 The Effects of the Discrete Fourier Transform

The problems found when the input parameters were not bin centred are caused because the computational method used differ from the expected idealised theory. Computationally, the discrete Fourier transform (DFT) is used, this gives a different result to the one that was expected when the continuous Fourier transform was used. The continuous Fourier transform of a phase-modulated wave would give the result

$$D(\omega) = \sum_{n=-\infty}^{\infty} (-i)^n J_n(\Gamma) \delta(\omega - \omega_0 - n\Omega),$$

as displayed in Equation 7 in Appendix A. This is what the search method is based on. However, the DFT is actually computed, giving the more complex result

$$D(\omega) = \sum_{j=0}^{N-1} e^{i\left(\frac{2\pi j}{N}(\kappa-k) + i\Gamma \cos\left(\frac{\Omega T}{N}j\right)\right)}. \quad (4)$$

as shown in Equation 12 in Appendix B. The expected delta functions making up the sidebands in the ideal continuous case become Dirichlet Kernels. As this cannot be simplified in the same way that was expected in Appendix A, the result of the search is not consistent across all input parameters as was shown in Section 3.1 and is thus not as successful as was initially hoped.

4 Conclusion

A coherent search algorithm has been developed that is successful in identifying correct input parameters from simulated data. It can identify any carrier frequency, ω , and there are some limitations in finding modulation frequency, Ω , due to characteristics of the Discrete Fourier transform. It has been suggested that these can be considerably improved by increasing the number of searches performed over Ω as shown in Section 3.1, though this comes at a significantly greater computational cost and would have to be investigated further.

The searches are convolution based, where the convolution is performed between the data in frequency space, which has only been Fourier transformed once, and its expected modulated form. The search is expected to be comparable in terms of robustness to noise and computational speed to other CW algorithms when searching over some parameters, however this is yet to be tested. The results should be scaled so this is possible.

It has been shown that the distance necessary between searches over Ω is over 1000 times more closely spaced more than for ω . However, the expected range of Ω is a lot smaller than for ω , therefore both searches could have a similar number of data points eventually. This needs to be carefully considered with respect to the computational time necessary to complete the entire search. In the future these tests should be repeated with Γ , though from previous results it is understood that the density of searches needed is significantly reduced in comparison to that for ω and Ω [1][5].

Acknowledgements

My mentor, Dick Gustafson, guided and inspired me throughout this program and I am immensely thankful for his support. I am very grateful for the time everyone at the LIGO collaboration and the other students spent with me, I have learnt so much from them. Additionally, I would like to thank the National Science Foundation and the Caltech SURF program for making it possible for me to complete this project.

References

- [1] Deanna Emery, 2015, ‘A Coherent Three Dimensional FFT Based Search Scheme for Gravitational Waves from Binary Neutron Star Systems’.
- [2] J.G. Martinez et al, 29 Sept 2015, ‘Pulsar J0453+1559: A Double Neutron Star System with a Large Mass Asymmetry’, *Astrophys.J.* 812 (2015) no.2, 143. page 3.
- [3] J.M. Lattimer, 15 May 2013, ‘The Nuclear Equation of State and Neutron Star Masses’, Stony Brook University, pages 55-57.
- [4] Discussions with Ansel Neunzert (University of Michigan) about the X-statistic method in TwoSpect.
- [5] Curtis Rau, 2016, ‘A Coherent Search for Frequency Modulated Waves’.
- [6] Robert Naeye, 23 August 2007, ‘Neutron Stars’, NASA, URL: <http://www.nasa.gov/missionpages/GLAST/science/neutronstars.html>
- [7] Binary Research Institute, ‘Binary Star Prevalence’, accessed August 2016, URL: <http://www.binaryresearchinstitute.org/bri/research/evidence/prevalence.shtml>
- [8] R G Lyons, 2001, ‘Understanding Signal Processing’, PH PTR, pages 71- 89.

A Derivation of Search Algorithm

The main concepts behind this algorithm were created in 2015 by Deanna Emery [1], below is the full derivation with additional notes.

The phase modulated gravitational wave, as is expected to be produced by a neutron star with a binary companion, is of the form

$$d(t) = e^{i(\omega_0 t + \Gamma \cos(\Omega t))}. \quad (5)$$

It is dependant on carrier frequency, ω , modulation frequency, Ω , and modulation index, Γ . Additionally, there are phase factors which have not been included here for simplicity but could be included in the future with minimal adjustments to the algorithm.

After factorization of the carrier ($e^{i\omega_0 t}$) and modulation ($e^{i\Gamma \cos(\Omega t)}$) terms and a rearrangement,

$$d(t).e^{-i\Gamma \cos(\Omega t)} = e^{i\omega_0 t}$$

can be obtained. The Fourier transform of both sides of the equation is then taken:

$$\text{FT}\{d(t).e^{-i\Gamma \cos(\Omega t)}\} = \text{FT}\{e^{i\omega_0 t}\}.$$

Using the Convolution principle,

$$\text{FT}\{A.B\} = \text{FT}\{A\} * \text{FT}\{B\},$$

the equation can be re-written as

$$\text{FT}\{d(t)\} * \text{FT}\{e^{-i\Gamma \cos(\Omega t)}\} = \text{FT}\{e^{i\omega_0 t}\}.$$

Then, using the Jacobi-Anger expansion,

$$e^{i\Gamma \cos(\Omega t)} = \sum_{n=-\infty}^{\infty} i^n J_n(\Gamma) e^{in\Omega t},$$

the equation becomes

$$D(\omega) * \text{FT}\left\{\sum_{n=-\infty}^{\infty} (-i)^n J_n(\Gamma) e^{in\Omega t}\right\} = \text{FT}\{e^{i\omega_0 t}\}, \quad (6)$$

where $D(\omega)$ is the normalised Fourier transform of the data, $d(t)$, at ω and $J_n(\Gamma)$ is the value of the n th Bessel function at Γ .

The Bessel functions play a strong role in determining the signal's side-bands in the frequency domain. It can be seen in Figure 5 that the largest magnitude Bessel term occurs when n is just less than Γ ; causing the sidebands of the signal's FFT to be largest at $n \approx \Gamma$. This can be physically interpreted as the neutron star spending the longest amount of time travelling directly towards or away from the earth, thus emitting the GW's with the largest (or smallest) Doppler shifts which are analogous to frequencies at the outermost sidebands.

The expected signal is

$$D(\omega) = \sum_{n=-\infty}^{\infty} (-i)^n J_n(\Gamma) \delta(\omega - \omega_0 - n\Omega). \quad (7)$$

However, this is true in the ideal continuous domain where all values of ω exist. Otherwise, it can be seen that $D(\omega)$

will always be equal to zero when the values of ω_0 and $n\Omega$ are not multiples of a bin (ω): which will always be the case experimentally as they will be irrational values. This is further discussed in Appendix B.

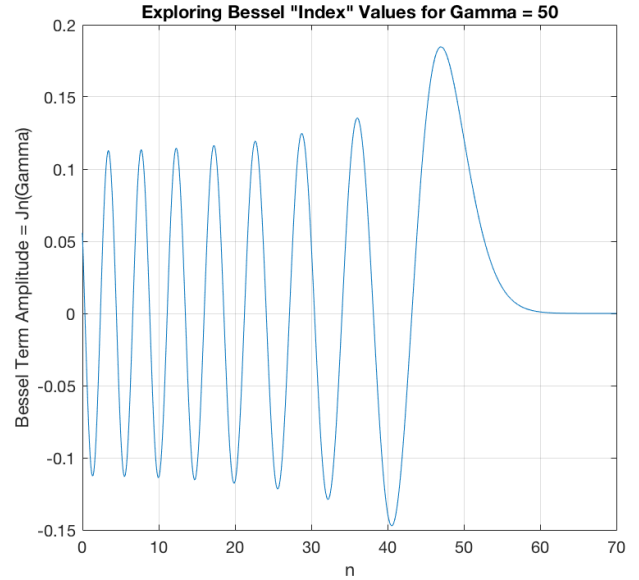


Figure 5: Figure displaying how the values of the Bessel terms depend on the index, n , where the amplitude computed is $J_n(\Gamma)$ and gamma is held constant at $\Gamma = 50$.

As the Fourier transform of $e^{in\Omega t}$ is $\delta(\omega - n\Omega)$, the convolution in Equation 6 picks out only these values of $D(\omega)$:

$$\sum_{n=-\infty}^{\infty} (-i)^n J_n(\Gamma) (D(\omega - n\Omega)) = \delta(\omega - \omega_0)$$

This assumes that the Fourier transform computed is continuous. This is not actually the case as a discrete Fourier transform has to be used because the input data is sampled to make a series of discrete time domain information. Additionally, only theoretically can an infinitely long time domain exist, this is not comparable to the finite lengths of a real data set. This assumption is expected to be the cause of extra phase terms which are so far unaccounted for and cause problems when searching over the modulation frequency. The actual expected output is discussed in Appendix B.

Assuming the continuous Fourier transform, by rearrangement of Equation 5,

$$J_0(\Gamma)D(\omega) + \sum_{n=1}^{\infty} e^{-in\frac{\pi}{2}} J_n(\Gamma) (D(\omega - n\Omega) + D(\omega + n\Omega)) = \delta(\omega - \omega_0) \quad (8)$$

is obtained. This used in the search, where the left hand side of this equation is repeatedly computed for different values of ω , Ω , and Γ . When the three parameters are correct, the value of the computed summation should be 1; as all the power from each frequency bin (side-band), previously normalised, is included. If this is not the case the value should approach 0. Therefore the correct parameters can be identified.

There is an additional phase term in the signal, $(-i)^n$, which rotates the sidebands rapidly through the complex plane. Accounting for this and the sign due to the Bessel term is the reason the search is coherent. If any of the trial parameters, ω , Ω or phase, are incorrect, the phases in the sum (Equation 8) will not add constructively causing very little signal to be recorded. Therefore, identifying the correct parameters is clear. This is an advantage to my other CW methods which use the magnitude of the FFT with no phase terms, however is additionally cause of the issues discussed in Appendix B.

B The Discrete Fourier Transform

The expected phase modulated gravitational wave has the form

$$d(t) = e^{i(\omega_0 t + \Gamma \cos(\Omega t))}. \quad (9)$$

However, the data is sampled, not taken continuously, leading to only discrete values of time, t_j . These can be relabelled using the time domain index, j , so that

$$t_j = j\Delta t = j\frac{T}{N}.$$

To keep notation consistent, ω_0 will also be relabelled with κ :

$$\omega_0 = 2\pi f_0 = \frac{2\pi\kappa}{T}.$$

It should be noted that as ω_0 can take any value, κ as not expected to be an integer. Equation 9 can then be written as

$$d(t) = e^{i\left(\frac{2\pi\kappa}{N}j + \Gamma \cos\left(\frac{\Omega T}{N}j\right)\right)}. \quad (10)$$

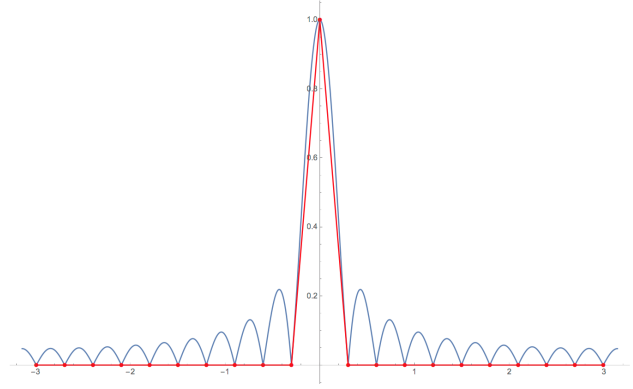
The discrete Fourier transform (DFT) is computed when taking the Fast Fourier transform (FFT) of data in the search algorithm. Explicitly it is

$$D(\omega) = \sum_{j=0}^{N-1} d(t) e^{-i2\pi jk/N}, \quad (11)$$

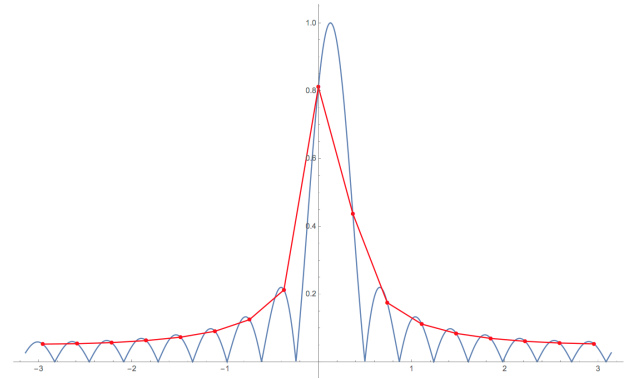
where k is the index of the current bin the DFT is being computed in, analogous to κ however always an integer:

$$\omega = 2\pi f = \frac{2\pi k}{T}.$$

If a simple oscillatory wave was the imputed data, for instance $d(t) = e^{i\omega_0 t}$, then the DFT (Equation 11) would be a Dirichlet kernel as seen in Figures 6a and 7. When ω_0 is centred on a frequency bin, all bins apart from ω_0 have a zero value and an overall delta function is seen. However, if ω_0 is not centred on a frequency bin, which is expected due to real life irrational inputs, the Dirichlet kernel is shifted so that the frequency bins measure non-zero values, this is undesirable and known as leakage [8]. This effect is illustrated using the magnitude of the Dirichlet kernel in Figure 6: where Figure 6a is the ideal bin centred result, and Figure 6b displays the leakage seen when ω_0 is off centred. The magnitude of the peak returned by the search is reduced if leakage occurs, reducing the searches robustness to noise. As seen in figure 7, there is additionally phase terms in the



(a) When ω_0 is bin-centred, it is sampled as a delta function. This is because the centre of each bin aligns with a zero of the Dirichlet kernel.



(b) When ω_0 is not bin-centred, leakage occurs. This is because the centre of each bin aligns with a non-zero value of the Dirichlet kernel. Therefore the FFT returned is misleading and power is lost in the search.

Figure 6: Sampling the magnitude of the Dirichlet kernel (in blue) at the centre of each bin (in red) with the ω_0 either bin-centred (a), or not (b). Images from [5].

kernel which significantly complicate the algorithm which is so reliant on phase information because it is coherent.

The phase modulated discrete data set, Equation 10, can be inserted into Equation 11 to find that the DFT of the expected phase modulated signal would be

$$D(\omega) = \sum_{j=0}^{N-1} e^{i\left(\frac{2\pi\kappa}{N}j + \Gamma \cos\left(\frac{\Omega T}{N}j\right)\right)} e^{-i2\pi jk/N}.$$

This can be simplified to

$$D(\omega) = \sum_{j=0}^{N-1} e^{i\left(\frac{2\pi j}{N}(\kappa - k) + \Gamma \cos\left(\frac{\Omega T}{N}j\right)\right)}, \quad (12)$$

which is plotted in Figure 8. This is a problem as the j term cannot be easily separated as in Equation 6, so a simplified sum cannot be made.

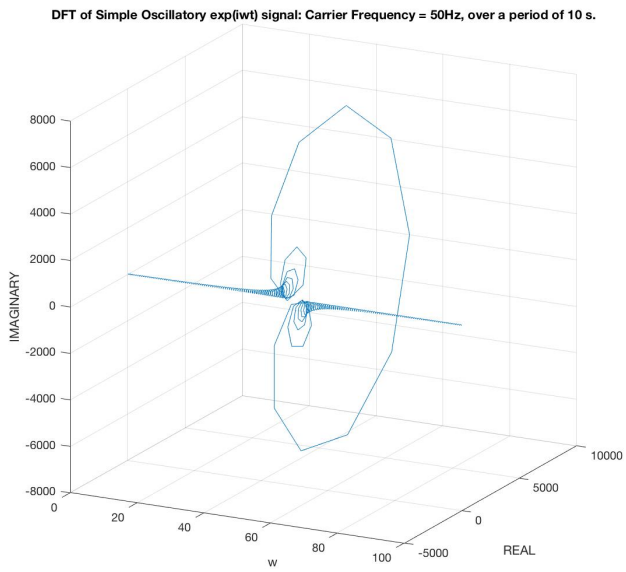


Figure 7: Figure displaying the DFT of a $e^{i\omega_0 t}$ signal in the complex plane. It should be noted how rapidly the phase of the signal changes about the midpoint ($\omega_0 = 50\text{Hz}$).

DFT of Phase Modulated Signal in Complex Plane: Carrier Frequency = 50, Modulation Frequency = 3, Gamma = 10 over a period of 1000 s.

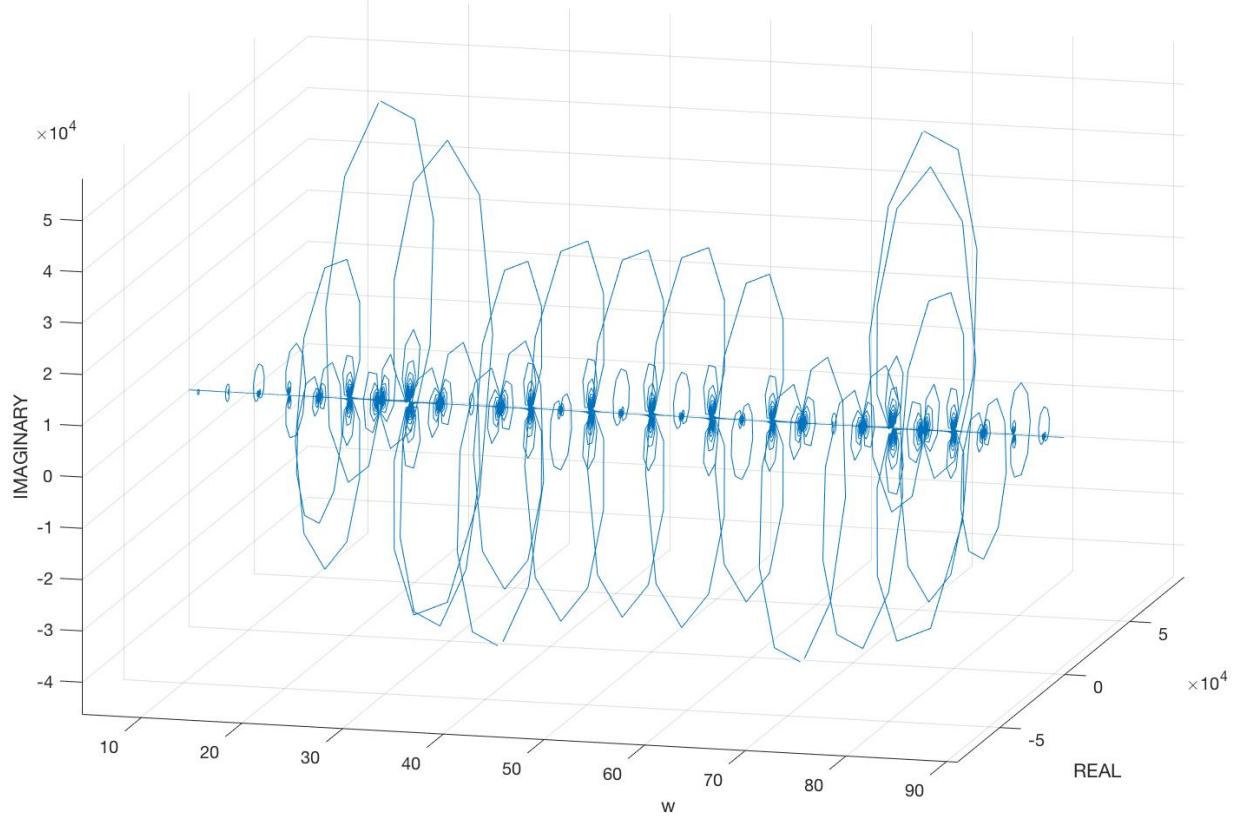


Figure 8: Figure displaying the expected complex DFT of a phase modulated signal, computed using Equation 12, with $\omega_0 = 50\text{Hz}$, $\Omega = 3\text{Hz}$ and $\Gamma = 10$.